PHYSICAL REVIEW D VOLUME 21, NUMBER 11 1 JUNE 1980

Experimental determination of elastic and topological cross sections in 48.9-GeV/c $\bar{p}p$ interactions

D. E. Zissa, V. E. Barnes, D. D. Carmony, L. J. Dauwe, J. A. Gaidos, L. J. Gutay, A. T. Laasanen, R. L. McIlwain, D. H. Miller, L. K. Rangan, R. M. Robertson,* and R. B. Willmann
Department of Physics, Purdue University, West Lafayette, Indiana 47907

F. Turkot
Fermi National Accelerator Laboratory, Batavia, Illinois 60510
(Received 24 September 1979)

The elastic and topological $\bar{p}p$ cross sections have been measured at 48.9 GeV/c in the Fermilab proportional-wire-chamber–30-in.-bubble-chamber hybrid spectrometer. The elastic cross section is 7.81 ± 0.24 mb and the slope of the elastic differential cross section at $t=0$ is 13.4 ± 0.8 GeV^{-2}. Further, the moments of the inelastic topological-cross-section distribution are $\langle n_c \rangle = 5.69 \pm 0.03$, $\langle n_c \rangle / D = 2.10 \pm 0.02$, and $f_2^{cc} = 1.67 \pm 0.12$.

I. INTRODUCTION

The nature of high-energy antiproton-proton interactions and their relation to proton-proton interactions are not yet fully understood.[1] Until recently, experimental study of $\bar{p}p$ interactions at high energies has been hindered by the unavailability of $\bar{p}$ beams. Moreover, the annihilation process becomes increasingly difficult to study as its cross section falls rapidly with increasing energy. The former difficulty has been overcome with an enriched $\bar{p}$ beam, and the study of high-energy $\bar{p}p$ annihilation has been optimized by choosing 50 GeV/c beam momentum, where the annihilation process is expected to be greater than 10% of the total $\bar{p}p$ cross section and where hadronic interactions are entering the high-energy regime. In this paper we present a study of some features of the $\bar{p}p$ charged-multiplicity distribution at 50 GeV/c and make comparisons with $\bar{p}p$ and pp interactions at energies between 3 and 400 GeV. In the accompanying paper we discuss the $\bar{p}p$-pp topological-cross-section differences.

II. APPARATUS AND DATA ANALYSIS

The results are derived from a sample of 92 000 pictures taken in the Fermilab proportional-wire-chamber–30-in.-bubble-chamber hybrid spectrometer (PWHS) (Ref. 2). The beam incident upon the hydrogen-filled rapid-cycling bubble chamber was created by a novel antiproton enrichment scheme, first proposed by Neale,[3] which was modified for greater $\bar{p}$ yield.[4] The 400-GeV/c extracted proton beam from the accelerator was focused onto a copper target located halfway along the bore of a 10-ft-long sweeping magnet which removed all charged particles emerging from the target. $\bar{\Lambda}$'s and other neutral particles that decayed, after emerging from the magnet at 6 mr, were the source of the beam which contained 30% antiprotons. The remainder of the beam consisted primarily of negative pions from the decay of K^0's and Λ^0's. A bubble-chamber photograph was taken only if two or more antiproton beam particles entered the chamber, resulting in an effective flux of ~42% antiprotons. As a result of this antiproton enrichment scheme, 57% of the observed interactions were induced by antiprotons.

The antiprotons were tagged by a Čerenkov counter operated in a threshold mode, and the antiproton events contain a 3% background from mistagged pion-induced events.[5] Three triplets of upstream proportional wire chambers (PWC's) accurately determined the beam position and direction in the bubble chamber. The beam momentum was determined to be 48.9 ± 0.5 GeV/c by swimming 1700 beam tracks from the upstream PWC's through the bubble-chamber magnetic field to the downstream wire chambers, as in Ref. 6. The quoted error in the beam momentum is dominated by uncertainties in the magnetic fringe field.

Events of all topologies, including those with V^0's and γ's pointing to the event vertex, were scanned and measured using scanning and measuring projectors with on-line three-view geometry program (TVGP). An effective track-reconstruction efficiency of approximately 99% was obtained with this system. A second independent scan was done on 20% of the film distributed evenly throughout the experiment. Separate single-scanning efficiencies were found for the following categories: zero-prong events without associated neutrals [(75 ± 25)%], two-prong events without associated neutrals [(85 ± 2)%], and all other events [(91 ± 1)%].

The ionization bubble density of each measured positive track with momentum less than 1.33 GeV/c was examined in order to obtain identification of slow protons and pions. The tracks unidentifiable by ionization were treated as pions unless they were otherwise identified by a four-constraint kinematic fit. No conflict was found between kinematic fits to elastic scattering (see below) and the bubble-density identification.

The four downstream PWC's located 2 to 6 m from the center of the bubble chamber utilized the bubble-chamber fringe field and the increased lever arm to improve the momentum measurement of fast secondary tracks. The proportional-wire geometry program (PWGP) (Ref. 7) was used to construct upstream and downstream wire-chamber tracks. The program HOOKUP (Ref. 8) was used to combine the bubble-chamber and wire-chamber data. An event was called a tagged $\bar{p}$ event only if the bubble-chamber beam track matched in intercept and angle with an upstream wire-chamber track associated with a null Čerenkov signal. Wherever possible, links were established between secondary tracks in the bubble chamber and the downstream PWC's when the bubble-chamber measured momenta were greater than 15 GeV/c. About 45% of the tracks with measured momenta between 15 and 25 GeV/c and about 70% of the tracks with measured momenta above 25 GeV/c were successfully linked with secondaries. The momentum resolution was 7–10% for the linked secondaries. The bare bubble-chamber information was used if there was no hookup.

III. DETERMINATION OF THE ELASTIC CROSS SECTION

The elastic reaction hypothesis was tried for all 2569 measured two-prong events using the SQUAW kinematic-fitting program. Instead of the usual four-momentum conservation, SQUAW was modified to conserve $\vec{p}$ and $E - \vec{p}\cdot\hat{n}$, where $\hat{n}$ is a unit vector in the incident-beam direction. Events having a four-constraint (4C) χ^2 of less than 30 were selected as elastic events. A few of the true elastic events failed to satisfy the above criterion after the first pass of measurements. In order to find additional candidates for elastic events, a remeasurement list was made (a) from the high-χ^2 tail of the 4C elastic distribution, (b) from 3C elastic fits where the momentum of the fast track was deleted, (c) from 4C fits obtained by dropping one of the three stereoscopic views, and (d) from events having a downstream wire hit compatible with the calculated direction of the fast elastic recoil track. Events which passed the 4C criterion after remeasurement were added to the elastic sample. This procedure resulted in a 10% addition to the initial elastic sample. Criterion (d) alone yields an 8% addition to the initial elastic sample.

To determine the elastic cross section and the total number of events, the following corrections were made:

(1) The inelastic event background in the sample selected as elastic events was measured as follows: (a) The contamination from multineutral events was found to be negligible after attempting to fit four-prong events with two tracks omitted. (b) It was found that two of the two-prong events with associated γ's passed the elastic selection criterion. Assuming that one π^0 was produced in each event and using the probability of pair conversion in the bubble chamber, a total contamination of $(2.4 \pm 1.7)\%$ was calculated.

(2) Both elastic and inelastic two-prong events with small four-momentum transfer squared (t) tended to be missed in both scans if the recoil proton track pointed toward or away from the cameras. Therefore, the distributions of the proton azimuthal angle about the beam direction were repopulated separately for the five t intervals in the range $0.04 \leq -t \leq 0.14$ GeV^2.

(3) In order to determine the number of elastic events with $-t \leq 0.04$ GeV^2, the elastic differential distribution was fitted to the form $A \exp(Bt + Ct^2)$ in the interval $0.04 \leq -t \leq 0.30$ GeV^2.

(4) After the initial fit and the low-t correction were made, the resulting total number of events was used along with $\sigma_T = 43.86 \pm 0.25$ mb (Refs. 9 and 10) and the optical theorem to compute the number of events (dN_{el}/dt) at $t = 0$. Imposing the condition that the fit passes through this point

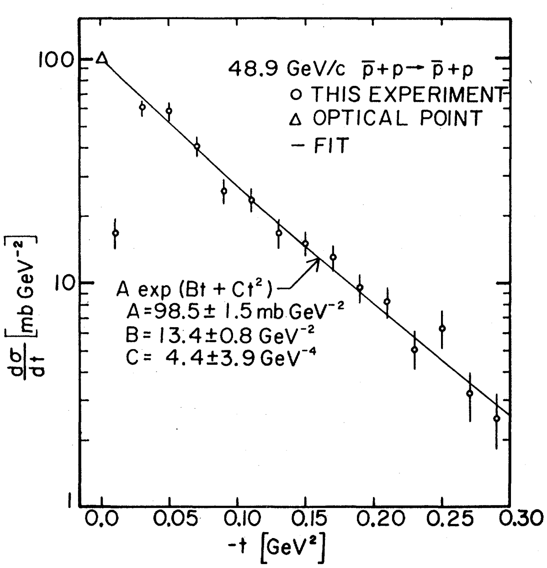

FIG. 1. Elastic differential cross sections $d\sigma/dt$. The optical point is calculated from the total cross section of Ref. 9. The fit, which is described in the text, does not include our two data points nearest to $t = 0$.

within its error of 1.5% relative to our data, the above procedure was iterated until consistency was obtained.

Using these procedures, the elastic and topological cross sections were obtained,[10] normalized to the above total cross section from Ref. 9. In particular, it was found that $\sigma_{el} = 7.81 \pm 0.24$ mb, where the uncertainties in all of the corrections have been folded in. The fitted parameters are

$$A = 98.5 \pm 1.5 \text{ mb GeV}^{-2},$$

$$B = 13.4 \pm 0.8 \text{ GeV}^{-2},$$

$$C = 4.4 \pm 3.9 \text{ GeV}^{-4}.$$

Figure 1 shows the elastic data along with the fit. The value of A reflects the optical point and therefore the counter data. The values of B and C reflect the data of this experiment and agree well with the parameters measured by Ayres *et al.*[11] A separate fit with C fixed at zero gave $B = 12.5 \pm 0.3$ GeV^{-2}.

IV. DETERMINATION OF MULTIPLICITY CROSS SECTIONS

First, corrections were made to each charged-multiplicity cross section for undetected Dalitz pairs. Neutral-strange-particle decays and γ conversions were measured, and constrained kinematic fits were attempted assuming that the neutral particles originated from the primary event vertex. γ's were weighted by the probability of converting in a cylindrical fiducial volume of radius 30 cm, and it was assumed that all γ's arose from π^0 decay and that the scanning efficiency for pairs was 100%. Using the π^0 Dalitz-decay branching ratio of 1.15%, it is estimated that about 200 out of 10 000 events have Dalitz pairs (for $\sim\frac{1}{3}$ of these events the Dalitz pair was found in scanning). The charged-multiplicity cross sections were adjusted according to the number of Dalitz pairs estimated in each topology.

Vees and γ conversions near the vertex can be confused with charged tracks at the vertex; however, it was determined that this effect is negligible: By comparing the number of vees and γ conversions found close to the event vertex (i.e., within cuts of 4, 2, 3, and 3 cm for γ, K^0, Λ, and $\bar{\Lambda}$, respectively) with the number found beyond the above cuts, it was determined that $\lesssim 0.3\%$ of the events would be affected.

Furthermore, no corrections were found necessary for unseen secondary interactions which produce extra charged tracks near the event vertex. Assuming an effective cross section of 40 mb for charged secondary interactions, it was determined that ~0.3% of these tracks would interact within 2 cm of the event vertex. This would affect ~1–5% of the 2–18-prong events, respectively. It is believed that most of these interactions have been detected in scanning by either charge imbalance or by tracks not pointing to the event vertex. Once detected most were discernible so that the uncertainties are smaller than the statistical errors on the number of events found. Such correction would be necessary only at higher energies where there are straighter tracks, smaller opening angles, and higher multiplicities.

Odd-prong events apparently not caused by secondary interactions were moved to the next higher multiplicity on the assumption that a short track was not visible.

V. DISCUSSION

All of the above corrections having been incorporated, the topological cross sections listed in Table I were obtained. The errors reflect the statistical uncertainties in the numbers of events found as well as the uncertainties in the above corrections and in the low-t elastic events. Also shown in Table I are moments of the inelastic charged-multiplicity distribution. Errors were computed using all correlation terms in the error matrix. In Fig. 2 the 48.9-GeV/c topological cross sections are plotted together with published data at different beam momenta.[12] The solid curves are to guide the eye. The zero-prong cross sec-

TABLE I. 48.9-GeV/c $\bar{p}p$ elastic and topological cross sections, and inelastic charged-multiplicity moments.

N_{charge}	Events found		Corrected number[a]	Cross section (mb)
0	32		43	0.149 ± 0.039
2	2569	elastic	2255	7.81 ± 0.24
		inelastic	1643	5.69 ± 0.22
4	2556		2985	10.34 ± 0.20
6	2236		2675	9.27 ± 0.19
8	1564		1852	6.42 ± 0.16
10	693		821	2.85 ± 0.11
12	258		287	0.994 ± 0.067
14	62		83	0.288 ± 0.036
16	15		12	0.042 ± 0.017
18	2		2.5	0.009 ± 0.007
⩾20	0		⩽2.7[b]	⩽0.009[b]
total	9987		12 658	43.86 ± 0.25[c]

$\langle n_c \rangle = 5.69 \pm 0.03$

$D \equiv (\langle n_c^2 \rangle - \langle n_c \rangle^2)^{1/2} = 2.71 \pm 0.02$

$\langle n_c \rangle / D = 2.10 \pm 0.02$

$\gamma \equiv \langle (n_c - \langle n_c \rangle)^3 \rangle / D^3 = 0.59 \pm 0.03$

$K \equiv \langle (n_c - \langle n_c \rangle)^4 \rangle / D^4 = 3.12 \pm 0.09$

$f_2^{cc} \equiv \langle n_c(n_c - 1) \rangle - \langle n_c \rangle^2 = 1.67 \pm 0.12$

[a] Corrections are explained in the text.
[b] Upper limit at 90% confidence level.
[c] From Ref. 9.

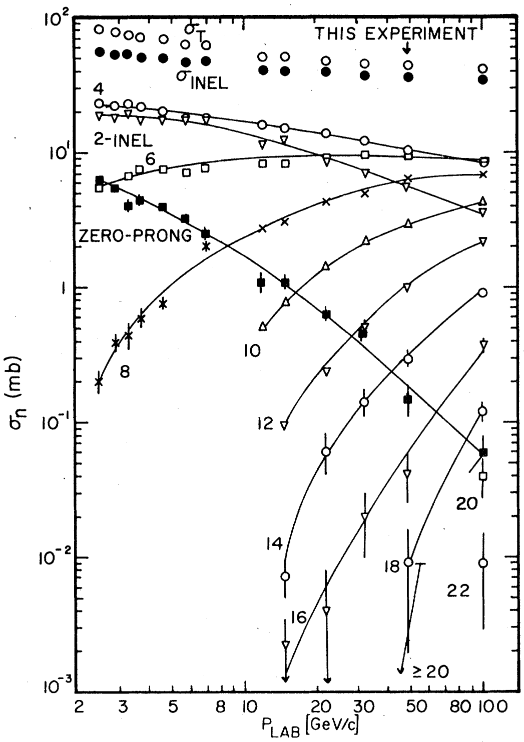

FIG. 2. $\bar{p}p$ total (σ_T), total inelastic (σ_{inel}), and topological cross sections (σ_n) as a function of laboratory beam momentum (Ref. 12). We show the upper limit at 90% confidence level for $\geqslant 20$ prongs calculated from 0 events found in our experiment. The curves are to guide the eye.

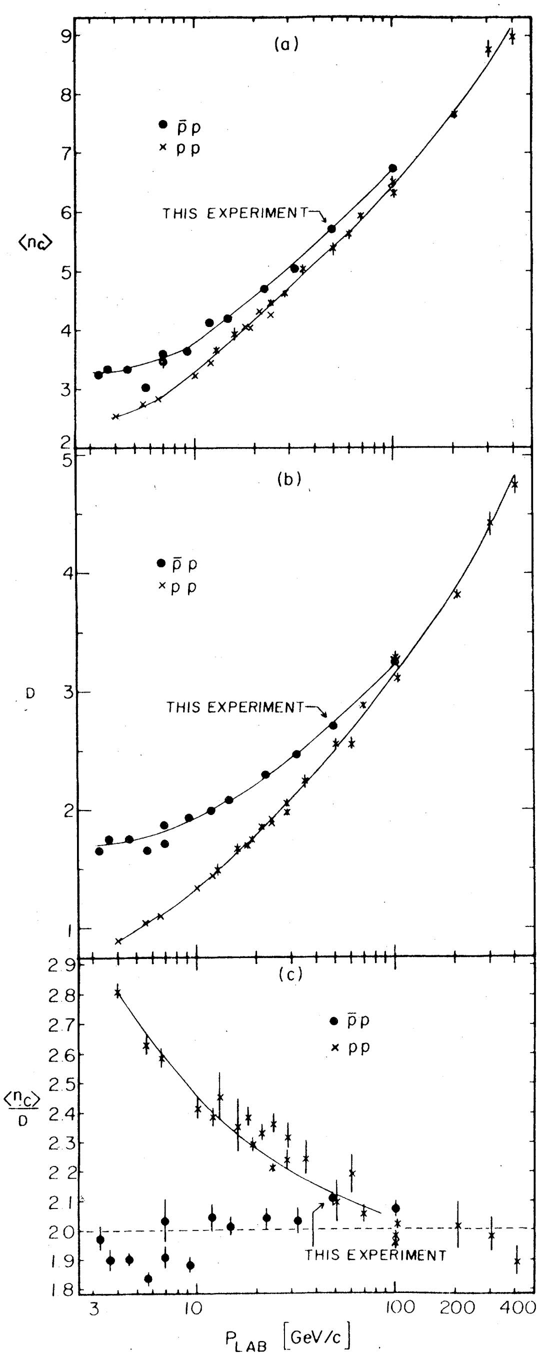

FIG. 3. (a) Average charged multiplicity $\langle n_c \rangle$, (b) dispersion D, and (c) the ratio $\langle n_c \rangle / D$ as a function of laboratory beam momentum for $\bar{p}p$ and pp inelastic interactions (Ref. 13). The curves are to guide the eye.

tion above 14 GeV/c is seen to decrease steeply as $\sim p_{LAB}^{-(1.45\pm0.14)}$. The 2- and 4-prong cross sections decrease monotonically with p_{LAB} over the whole range of the figure from 2.5 GeV/c up to 100 GeV/c. 8- and higher-prong cross sections rise monotonically, and are seen to continue to rise between 50 and 100 GeV/c. In particular, the 18- and 20-prong cross sections are rising very steeply at the highest measured energies.

The average charged multiplicity $\langle n_c \rangle$, the dispersion D, and the ratio $\langle n_c \rangle / D$ are shown in Figs. 3(a)–3(c) and are compared with data at a series of other momenta.[13] Our data fall on smooth curves through the previous data including the 32- and 100-GeV/c points. In the highest-measured momentum range, 50 GeV/c and above, the values of $\langle n_c \rangle$ for $\bar{p}p$ and for pp collisions may be slowly approaching each other, but higher-energy $\bar{p}p$ data are required to determine if they converge. The values of D apparently converge before 200 GeV/c, which may be caused in part by the decrease with energy of the annihilation component of the $\bar{p}p$ multiplicity distribution. The ratios $\langle n_c \rangle / D$ appear to have converged already by 50 GeV/c, and there are indications that the value for $\bar{p}p$ interactions may begin to exceed the value for pp interactions. In the region $3 \leqslant p_{LAB} \leqslant 50$ GeV/c, this ratio for $\bar{p}p$ interactions is approximately constant at ~2.0, although it is increasing slowly, whereas $\langle n_c \rangle / D$ for pp interactions is decreasing rapidly with increasing beam momentum.

We have compared our data to the Koba-Nielsen-Olesen (KNO) scaling curve (not shown) fitted to pp data between 50 and 303 GeV/c (Ref. 14). Our $\bar{p}p$ distribution is slightly narrower than the KNO curve fit for the high-energy pp data since the width $D/\langle n_c \rangle$ is smaller for our data.

A study of the difference between $\bar{p}p$ and pp topological cross sections will be presented in the following paper.

ACKNOWLEDGMENTS

We would like to thank S. Pruss, M. Johnson, and W. Neale for helping to carry out the 40–60 GeV/c $\bar{p}$-beam feasibility test. Further, we would like to thank L. Stutte and R. Stefansky for their help with the beam and D. Theriot for his interest and support. The cooperation of the neutrino laboratory technical staff in the design and fabrication of the target and associated vacuum system is appreciated. We express our gratitude to the Hybrid Spectrometer Consortium and in particular to R. K. Yamamoto, J. Brau, and A. Napier for maintaining their downstream chambers and the on-line computer during our experiment. Finally, we thank members of the Purdue scanning and measuring staff for their part in the analysis of the film. This research was supported in part by the United States Department of Energy.

---

*Present address: University of Oklahoma, Department of Physics and Astronomy, Norman, Okla. 73019.

[1]Y. Eylon and H. Harari, Nucl. Phys. B80, 349 (1974).

[2]D. Fong *et al.*, Phys. Lett. 53B, 290 (1974), and references therein; D. Fong *et al.*, Nucl. Phys. B102, 386 (1976), and references therein.

[3]W. W. Neale, Fermilab Report No. FN-259, 1974 (unpublished).

[4]V. E. Barnes *et al.*, Memo Nos. 350 and 351, High Energy Physics Notes, Purdue University, 1975 (unpublished).

[5]A comparison of the beam-tagging Čerenkov counter and another Čerenkov counter for the last quarter of the run showed that the antiproton signal included a 6% background (mostly consisting of negative pions). Taking into account π^- decay between the tagging Čerenkov and the bubble chamber and the $\pi^-/\bar{p}$ cross section ratio, a 3% background in the antiproton event sample was calculated.

[6]W. M. Bugg, University of Tennessee report, 1974 (unpublished); University of Tennessee, Newsnote No. 28, 1974 (unpublished).

[7]D. Fong, T. W. Ludlam, T. L. Watts, PHS Consortium Newsnote No. 36, 1973 (unpublished).

[8]J. T. Carroll, SLAC BC Note No. 16, 1972 (unpublished); W. M. Morse, thesis, Purdue University, 1975 (unpublished).

[9]A. S. Carroll *et al.*, Phys. Rev. Lett. 33, 928 (1974).

[10]The total cross section σ_T was determined to be 44.9 ± 1.2 mb, using 20% of the film. This result is in good agreement with that of Carroll *et al.* (Ref. 9), σ_T = 43.86 ± 0.25 mb at 50 GeV/c.

[11]D. S. Ayres *et al.*, Phys. Rev. D 15, 3105 (1977).

[12]2.45 and 2.9 GeV/c: R. J. Abrams *et al.*, Phys. Rev. D 1, 1917 (1970); D. L. Parker *et al.*, Nucl. Phys. B32, 29 (1971); P. S. Eastman *et al.*, *ibid.* B51, 29 (1973); 3.28 and 3.66 GeV/c: T. Ferbel *et al.*, Phys. Rev. 137, B1250 (1965); 4.6 GeV/c: E. Bracci *et al.*, Report No. CERN/HERA 73-1 (unpublished); D. Everett *et al.*, Nucl. Phys. B73, 449 (1974); 5.7 GeV/c: K. Böckmann *et al.*, Nuovo Cimento 42A, 854 (1966); 6.94 GeV/c: T. Kitagaki *et al.*, Phys. Rev. Lett. 21, 175 (1968); T. Ferbel *et al.*, Phys. Rev. 173, 1307 (1968); 12 GeV/c: W. Galbraith *et al.*, *ibid.* 138, B913 (1965); K. J. Foley *et al.*, Phys. Rev. Lett. 11, 503 (1963); I. Borecka *et al.*, Nuovo Cimento 5A, 19 (1971); 14.75 GeV/c: W. Galbraith *et al.*, Phys. Rev. 138, B913 (1965); K. J. Foley *et al.*, Phys. Rev. Lett. 11, 503 (1963); D. Birnbaum *et al.*, *ibid.* 23, 663 (1969); F. T. Dao *et al.*, Phys. Lett. 51B, 505 (1974); 22.4 GeV/c: E. Bracci *et al.*, Report No. CERN/HERA 73-1 (unpublished); Yu. M. Antipov *et al.*, Nucl. Phys. B57, 333 (1973); L. N. Abesalashvili *et al.*, Phys. Lett. 52B, 236 (1974); 32 GeV/c: S. P. Denisov *et al.*, Phys. Lett. 36B, 528 (1971); M. A. Jabiol *et al.*, Nucl. Phys. B127, 365 (1977); 100 GeV/c: A. S. Carroll *et al.*, Phys. Rev. Lett. 33, 928, 932 (1974); R. E. Ansorge *et al.*, Phys. Lett. 59B, 299 (1975).

[13]Compilation of inelastic charged-multiplicity data on $\pi^\pm$, $K^\pm$, p, and $\bar{p}$ interaction on hydrogen: E. De Wolf *et al.*, Nucl. Phys. B87, 325 (1975); 60 GeV/c pp: C. Bromberg *et al.*, Phys. Rev. D 15, 64 (1977); 100 GeV/c pp: W. M. Morse *et al.*, Phys. Rev. D 15, 66 (1977); 100 GeV/c $\bar{p}p$: R.E. Ansorge *et al.*, Phys. Lett. 59B, 299 (1975); J. Whitmore, Phys. Rep. 27C, 187 (1976); 12 GeV/c $\bar{p}p$: see Ref. 12.

[14]P. Slattery, Phys. Rev. D 7, 2073 (1973).